npj | vaccines

Article

Published in partnership with the Sealy Institute for Vaccine Sciences

https://doi.org/10.1038/s41541-026-01393-0

Evaluation of safety and efficacy of an auxotrophic *aroA* mutant live attenuated vaccine against piscine *Streptococcus agalactiae* infection

Meng Nie[1], Changming Guo[2], Yuhao Dong[1], Ting Xu[1], Yaru Sun[1] & Yongjie Liu[1] ✉

Streptococcus agalactiae is a major pathogen threatening global tilapia aquaculture, causing severe economic losses due to high mortality. The rise of antimicrobial resistance necessitates the development of effective vaccines for streptococcosis control. Here, we generated an auxotrophic mutant through the targeted deletion of the *aroA* gene, which encodes a key enzyme in aromatic amino acid biosynthesis. The *aroA* mutant (Δ*aroA*) exhibited reduced intracellular survival within macrophages, a phenotype that was not restored by supplementation with exogenous aromatic amino acids under our experimental conditions. These findings suggest that *aroA* contributes to intracellular survival through mechanisms extending beyond its role in aromatic amino acid biosynthesis. In zebrafish, Nile tilapia and mouse models, Δ*aroA* demonstrated stable attenuation, reduced endothelial cell damage, and mitigated blood-brain barrier disruption and neuroinflammation, confirming its safety. The Δ*aroA* strain provided dose-dependent protection against lethal *S. agalactiae* challenges in both tilapia and mice, with 100% protection in tilapia conferred at a dose of 10^6 CFU following intraperitoneal administration. This study represents the first investigation into the role of *aroA* in *S. agalactiae* pathogenicity, providing valuable insights into the mechanisms of micronutrient utilization during bacterial pathogenesis. Also, our findings strongly support auxotrophic mutation as a promising attenuation strategy for vaccine development against streptococcosis in aquatic species.

Streptococcus agalactiae (group B *Streptococcus*, GBS), a β-hemolytic Gram-positive pathogen, exhibits remarkable zoonotic potential with confirmed infections in diverse hosts, including humans[1,2], mammals[3,4], and aquatic species[5,6]. Tilapia ranked as the second most cultivated fish in the world, with global production exceeding 5.3 million tonnes in 2022[7]. China has become the largest producer and consumer of tilapia[8]. However, the rapid expansion of tilapia farming has been accompanied by severe disease outbreaks caused by GBS, particularly the hypervirulent sequence type 7 (ST7) strain prevalent in China[9,10]. GBS infections in tilapia manifest as acute meningoencephalitis and hemorrhagic septicemia[11,12], causing high cumulative mortality rates in affected farms that threaten to both food security and economic sustainability in major producing regions[13]. Although beta-lactam antibiotics remain the first-line treatment for *S. agalactiae* infections[14], increasing evidence reveals an alarming trend of decreased drug susceptibility to penicillin, erythromycin, levofloxacin, and clindamycin, and other antibiotics[15–18]. This antimicrobial resistance is further amplified by the transmission of antimicrobial resistance genes (ARGs) through aquaculture systems, creating a cycle that endangers both ecosystem integrity and human health[19,20]. Despite growing concerns, effective control measures for GBS infection remain limited[21].

Vaccination represents a promising approach for disease control in aquaculture. However, while inactivated vaccines offer superior safety, their application is limited by their unsuitability for small fish fry (approximately 5 g), whether administered by injection or immersion, posing a significant barrier to their widespread adoption in aquaculture[22]. As an alternative, live-attenuated vaccines have emerged as promising candidates for inducing

[1]MOE Joint International Research Laboratory of Animal Health and Food Safety, College of Veterinary Medicine, Nanjing Agricultural University, Nanjing, China. [2]Jiangsu Key Laboratory for High-Tech Research and Development of Veterinary Biopharmaceuticals, Jiangsu Agri-animal Husbandry Vocational College, Taizhou, China. ✉e-mail: liuyongjie@njau.edu.cn

protective immunity against bacterial diseases in fish[23]. This is supported by a recent meta-analysis of tilapia vaccination against *Streptococcus* infections, which demonstrated that attenuated vaccines provide the highest mean relative percentage survival (RPS)[24]. The conventional strategy for developing live attenuated vaccines involves attenuating highly virulent strains by deleting specific virulence factors[25–27]. Although these vaccines typically cannot disseminate or cause disease in competent hosts, they may pose a clinical safety risk due to potential reversion to virulence, particularly for immunocompromised individuals[28]. Also, there could be the concern that the loss of classical virulence factors may compromise the efficacy of primed immune responses. Engineered auxotrophic bacteria whose replication is dependent on a natural or unnatural metabolite not found in the host provide a good candidate for a live attenuated vaccine. Some reports indicated that auxotrophic mutations can effectively attenuate bacterial virulence while preserving the ability to induce a robust immune response[29–32]. Several studies have described the development of attenuated auxotrophic strains by deleting the *aroA* gene, which encodes 5-enolpyruvylshikimate-3-phosphate synthase (EPSPS) involved in the biosynthesis of aromatic amino acids[33], and demonstrated that these mutant strains could exhibit protective immunity against bacterial infections[34–36]. Recently, Sereme et al.[37]. developed an effective Δ*aroA* attenuated live vaccine in *Escherichia coli* K1, further supporting the potential of targeting the shikimate pathway for vaccine development.

In our previous study, we identified 60 distinct genes, including *aroA*, that were preferentially expressed in *S. agalactiae* during interaction with macrophages[38]. But the role of *aroA* in *S. agalactiae* virulence remains unclear. In this study, we characterized the attenuation phenotype of the Δ*aroA* strain, and evaluated its immunological properties in both mice and tilapia. Our findings provide substantial preclinical evidence supporting a novel vaccine development strategy against *S. agalactiae* infections, highlighting the potential of auxotrophic mutants as safe and effective vaccine candidates.

Results

Development of the *S. agalactiae* auxotrophic mutant Δ*aroA*

The shikimate pathway for the biosynthesis of chorismate in bacteria is depicted as Fig. 1A, as described by a previous report from Rafia et al.[39]. In this pathway, the *aroA* gene encodes an enzyme involved in the sixth step of the shikimate pathway. To investigate its role, we generated a marker-free, non-polar Δ*aroA* strain in the piscine *S. agalactiae* clinical isolate GD201008-001 using double-crossover homologous recombination. The complemented strain (CΔ*aroA*) was constructed by reintroducing the *aroA* gene via a shuttle cloning vector pSET2. Quantitative real-time reverse transcription-PCR (qRT-PCR) confirmed successful deletion and complementation (Fig. 1B).

Given that *aroA* is essential for the biosynthesis of chorismate, we characterized the growth rates of the *S. agalactiae* strains in two media, including nutrient-rich Todd-Hewitt broth (THB) and nutrient-limited Dulbecco's Modified Eagle Medium (DMEM). The Δ*aroA* exhibited growth comparable to the wild-type (WT) strain in THB but showed significant reduction in DMEM (Fig. 1C). This phenotype was rescued in the CΔ*aroA* strain. These findings suggest that *aroA*-mediated metabolism is critical for bacterial growth under nutrient-limited conditions.

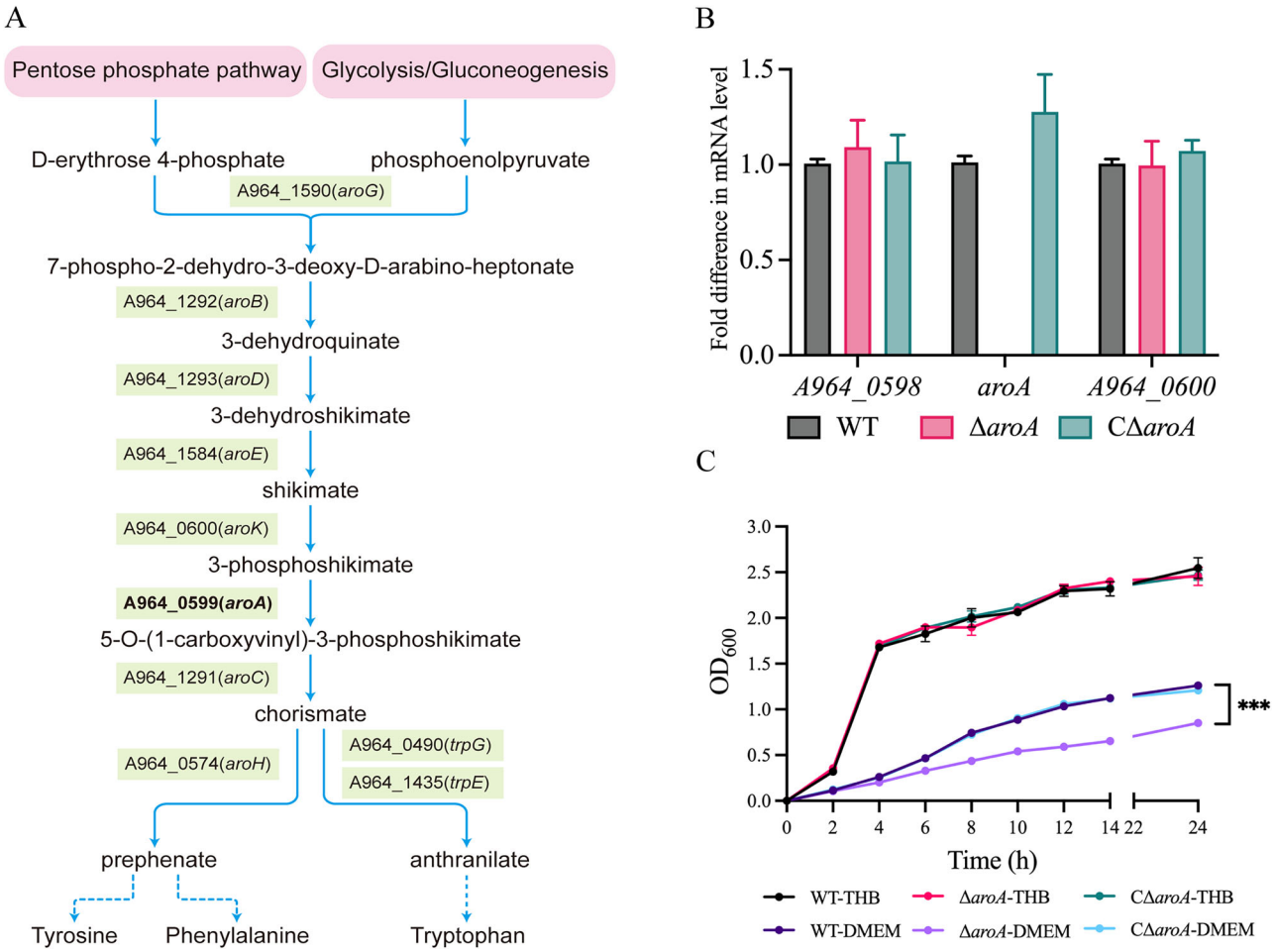

Fig. 1 | Identification and growth characteristics of the mutant strain Δ*aroA* and complement strain CΔ*aroA*. **A** Schematic representation of the shikimate pathway in *S. agalactiae*, with locus tags and gene names displayed in the boxes. **B** qRT-PCR analysis for expression of *aroA* and its flanking genes. **C** Growth curves of *S. agalactiae* strains in THB or DMEM medium at 37 °C, and the OD_{600} was measured every 2 h. Error bars represent standard deviation (SD). ***$P < 0.001$.

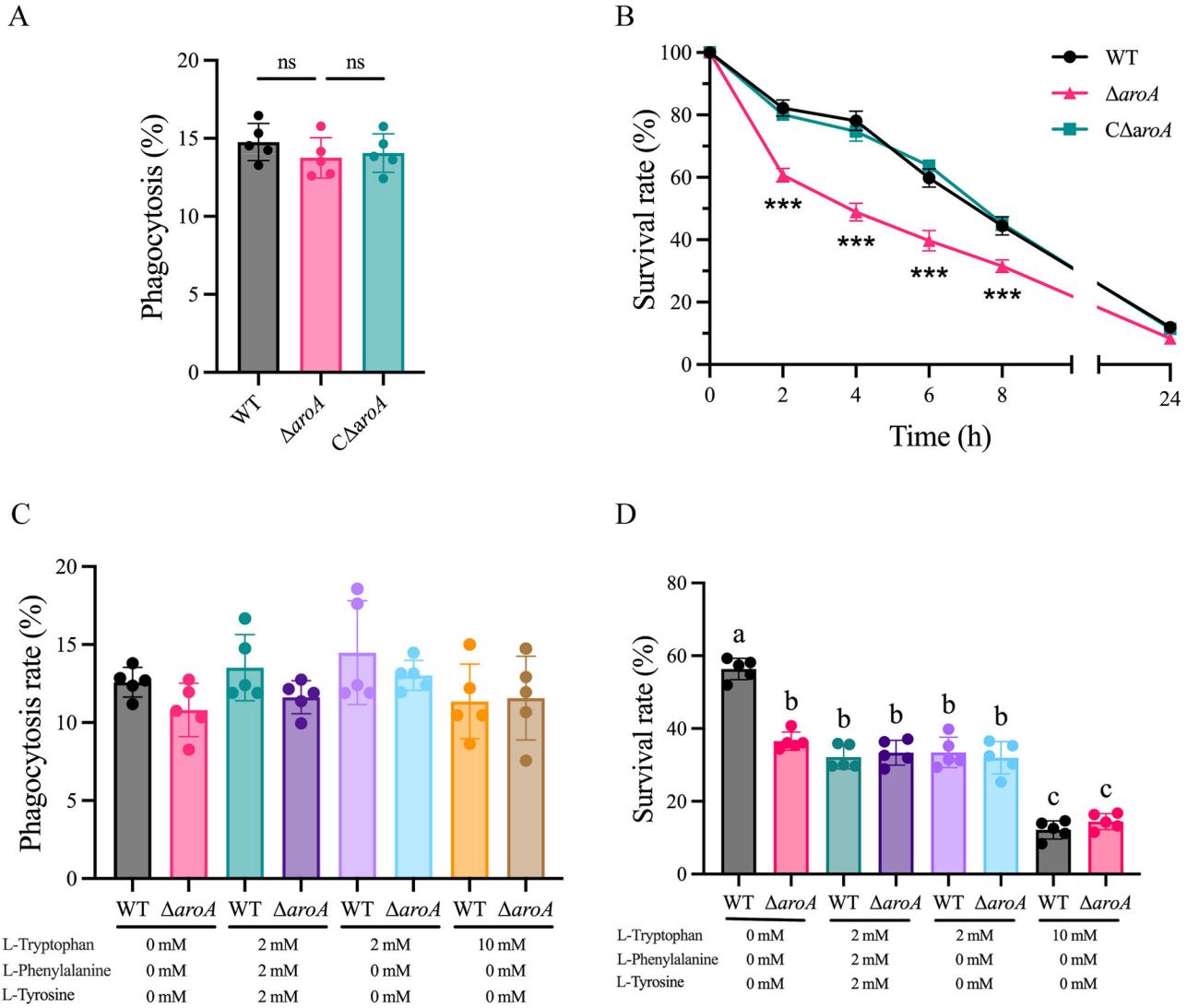

Fig. 2 | Impact of *aroA* deletion on intracellular survival of *S. agalactiae* in macrophages. A Phagocytosis rate of *S. agalactiae* strains by RAW264.7 macrophages, with intracellular bacteria quantified by CFU after 1 h infection and antibiotic treatment. **B** Intracellular survival of *S. agalactiae* in RAW264.7 macrophages at the indicated time points. Effects of aromatic amino acid supplementation on phagocytosis rate (**C**) and intracellular survival (**D**). Error bars represent SD. ***$P < 0.001$. Different lowercase letters indicate statistically significant differences between groups ($P < 0.05$).

Impact of *aroA* deletion on anti-phagocytosis and intramacrophage survival of *S. agalactiae*

Our previous study indicated that *aroA* was preferentially expressed in macrophages[38]. To evaluate its role in *S. agalactiae* virulence, we first investigated whether *aroA* contributes to bacterial resistance to phagocytosis and intracellular survival. Using murine macrophage RAW264.7 cells, we compared the phagocytic uptake and post-internalization persistence of WT, Δ*aroA*, and CΔ*aroA* strains. Notably, while the phagocytosis rate of the Δ*aroA* strain did not differ significantly from that of the WT or CΔ*aroA* strains (Fig. 2A), its intracellular survival was markedly impaired. At 2, 4, 6, and 8 h post-infection (hpi), the Δ*aroA* exhibited a significant reduction in bacterial survival compared to both the WT and CΔ*aroA* strains (Fig. 2B). These findings suggest that although *aroA* disruption does not affect initial macrophage uptake, it severely compromises bacterial persistence within phagocytes.

Considering that chorismate, the end product of the shikimate pathway, is the precursor for the aromatic amino acids tryptophan (Trp), phenylalanine (Phe) and tyrosine (Tyr)[40], we hypothesized that supplementation with the three aromatic amino acids might restore the intracellular survival defect of the Δ*aroA*. Unexpectedly, while phagocytosis rates remained unaffected (Fig. 2C), supplementation with all three aromatic amino acids or Trp alone reduced the survival of WT within macrophages and abolished its survival advantage over the Δ*aroA* (Fig. 2D). Consistent with this observation, in silico genome analysis suggested that *S. agalactiae* GD201008-001 lacks the genetic capacity for de novo synthesis of Trp, Phe, and Tyr, as indicated by a truncated *trp* operon (with only *trpEG* retained) and the absence of *pheA*, *tyrA* and *tyrB* orthologs (Fig. S2). Together, these data suggest that the intracellular survival defect of Δ*aroA* is not solely attributable to impaired aromatic amino acid biosynthesis under the conditions tested.

Characterizing the attenuation phenotypes of *S. agalactiae* Δ*aroA*

To evaluate the virulence of the Δ*aroA*, we employed well-established infection models in both aquatic and mammalian hosts. In zebrafish (*Danio rerio*), the Δ*aroA* strain showed remarkable attenuation, requiring challenge doses over 1000-fold higher than WT or CΔ*aroA* strains to achieve comparable mortality (Fig. 3A). The 50% lethal dose (LD_{50}) of Δ*aroA* was 3.97×10^5 colony-forming units (CFU) per fish, significantly higher than that of WT (1.71×10^2 CFU/fish) or CΔ*aroA* (3.27×10^2 CFU/fish).

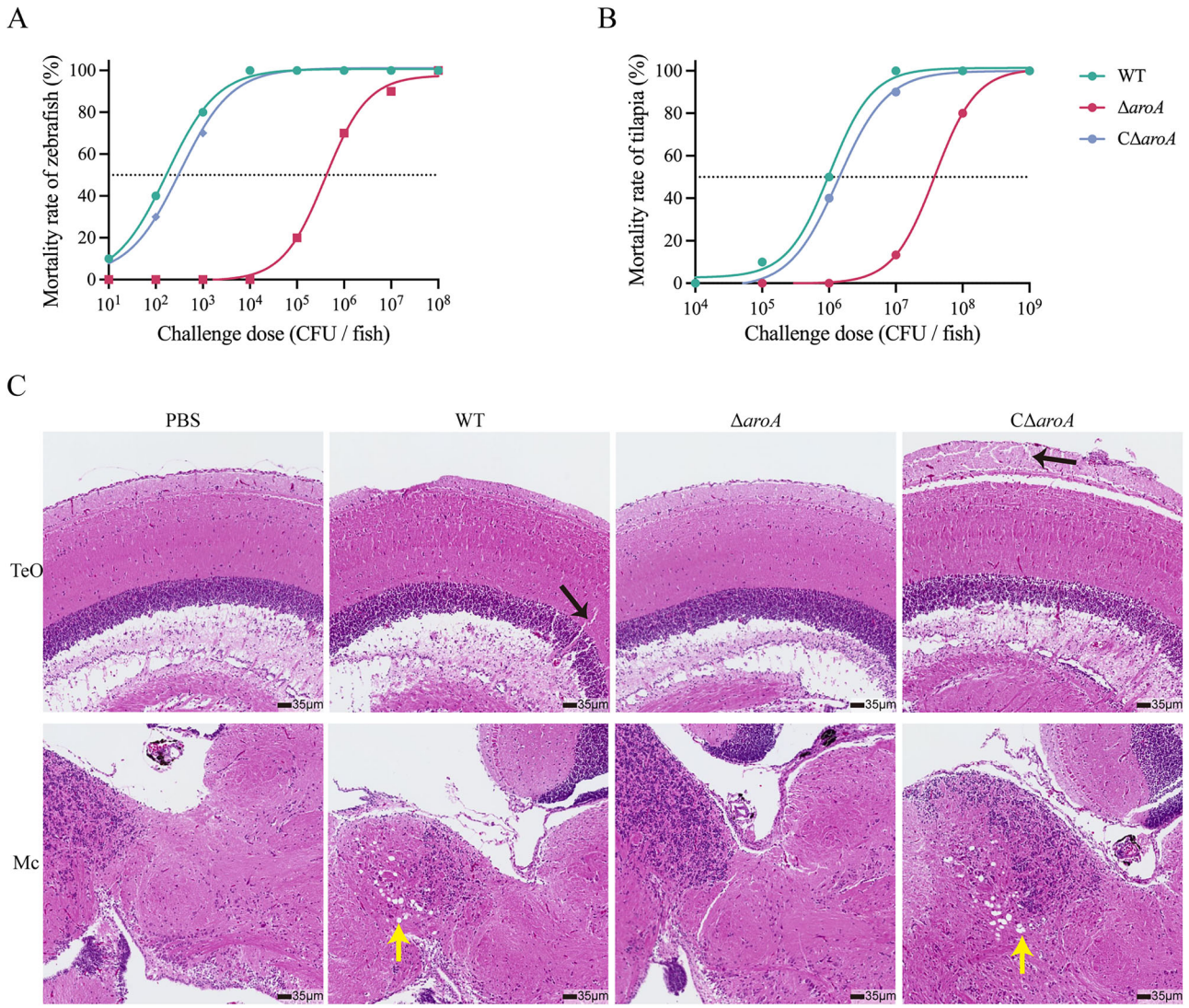

Fig. 3 | Attenuated virulence of the Δ*aroA* strain in teleost fish. A LD_{50} determination for *S. agalactiae* in zebrafish. **B** LD_{50} determination for *S. agalactiae* in Nile tilapia. **C** Histopathological lesions in H&E-stained brain tissues of Nile tilapia infected with the indicated *S. agalactiae*. Black arrows indicate fragmentation of the optic tectum organization, while yellow arrows indicate neuronal vacuolation (neuronal vacuolar degeneration). TeO the optic tectum, Mc mesencephalon.

Similarly, in the Nile tilapia (*Oreochromis niloticus*), the LD_{50} value of Δ*aroA* (2.51×10^7 CFU/fish) exceeded that of WT (1.03×10^6 CFU/fish) or complemented strains (1.38×10^6 CFU/fish) by one order of magnitude (Fig. 3B). Histopathological analysis further demonstrated that infection with WT and CΔ*aroA* strains led to fragmentation of the optic tectum organization and neuronal vacuolar degeneration in Nile tilapia (Fig. 3D). In contrast, the brain tissue of tilapia infected with Δ*aroA* remained relatively intact and smooth.

The attenuation of Δ*aroA* was further confirmed in a BALB/c murine meningitis model. All mice infected with either WT or CΔ*aroA* died within 28 hpi, whereas no death occurred inΔ*aroA*-infected mice, demonstrating the essential role of the shikimate pathway in bacterial pathogenesis (Fig. 4A). Quantitative analysis for the bacterial burdens revealed severely impaired systemic dissemination of the Δ*aroA*, demonstrating 3–4 log reductions in blood (Fig. 4B) and spleen (Fig. 4C), and complete absence from brain tissue (Fig. 4D) at 16 hpi, compared to WT and CΔ*aroA*. Further, histopathological analysis confirmed that, in contrast to Δ*aroA*-infected mice, WT- and CΔ*aroA*-infected mice exhibited significant histopathological lesions, including meningeal vascular congestion, hemorrhage and neuronal necrosis (Fig. 4E). These findings establish the *aroA*-mediated metabolism as an essential and conserved virulence determinant in *S. agalactiae* pathogenesis.

aroA contributes to endothelial damage, blood-brain barrier (BBB) disruption, and neuroinflammation

Using bEnd.3 brain microvascular endothelial cells, we compared the adhesion ability and cytotoxicity of *S. agalactiae* strains. Results demonstrated that the Δ*aroA* strain exhibited significantly reduced adhesion relative to WT or CΔ*aroA* strain (Fig. 5A). Additionally, lactate dehydrogenase (LDH) release assay revealed that infection with Δ*aroA* caused significantly reduced cell lysis, indicating a diminished capacity for endothelial damage (Fig. 5B). Further, we employed an Evans Blue (EB) dye-based assay to quantify BBB permeability during *S. agalactiae* infection. Infections with WT and CΔ*aroA* led to significant BBB disruption at 16 hpi, whereas mice infected with the Δ*aroA* strain maintained BBB integrity comparable to uninfected controls until 72 hpi (Fig. 5C).

Given the established role of IL-1β, IL-6, and TNF-α as the principal biomarkers of bacterial meningitis[41,42], we assessed neuroinflammatory responses in the murine model. Brain tissues from Δ*aroA*-infected mice exhibited significantly attenuated expression of all three proinflammatory cytokines compared to WT- and CΔ*aroA*-infected groups at both 10 and

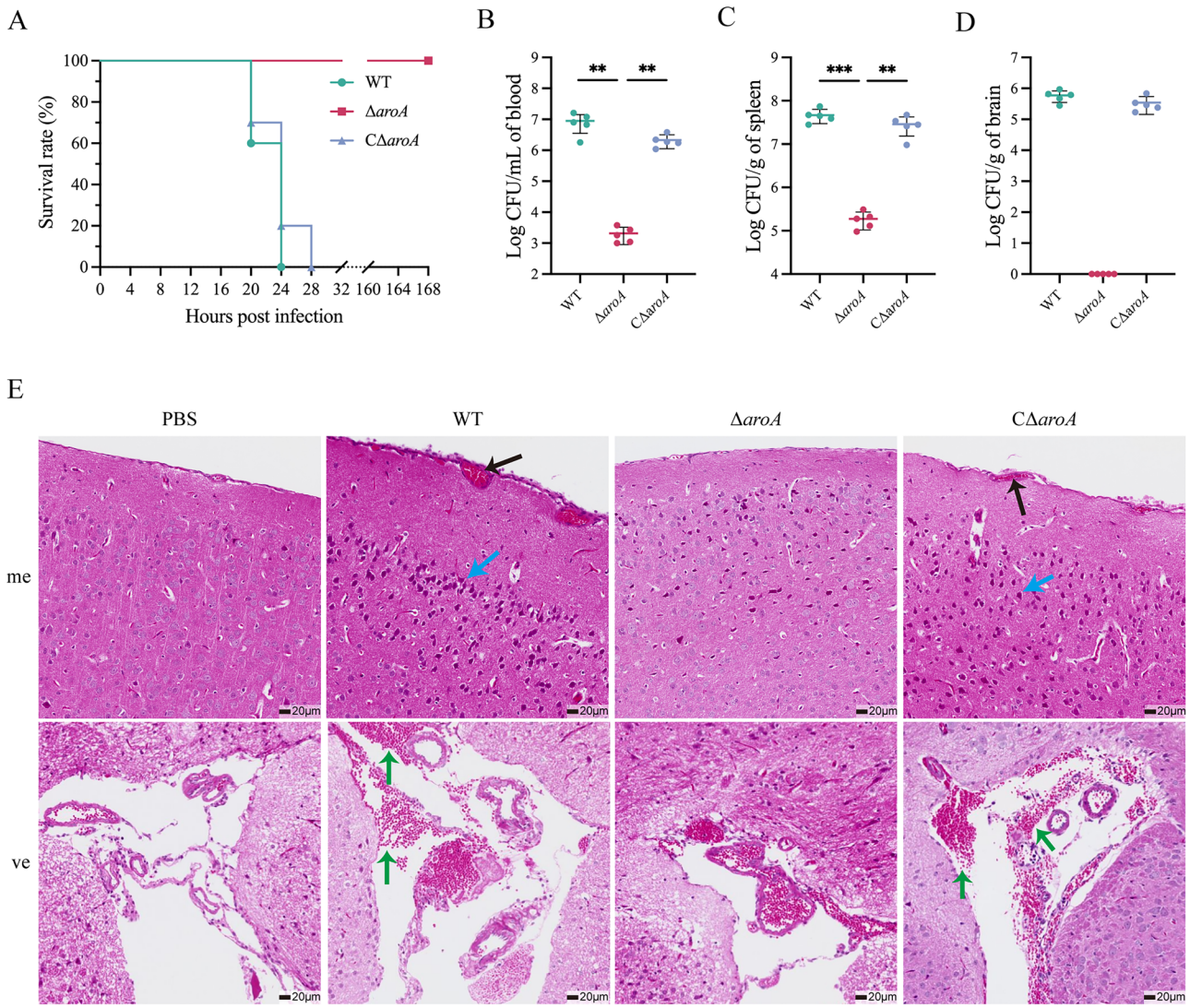

Fig. 4 | Attenuated virulence of the Δ*aroA* strain in BALB/c mice. A Kaplan–Meier survival curve of mice infected with 100 CFU indicated *S. agalactiae* strain ($n = 10$). Bacterial loads in bloods (**B**), brains (**C**), spleens (**D**) ($n = 5$). **E** Histopathological lesions in H&E-stained brain tissues of mice infected with the indicated *S. agalactiae*. The blue arrows indicate neuronal coagulative necrosis, green arrows indicate vascular hemorrhage and black arrows indicate vascular congestion. me meninges, ve ventricle. Error bars represent SD. $^{**}P < 0.01$; $^{***}P < 0.001$.

15 hpi (Fig. 5D–F). These results highlight that *aroA*-mediated metabolic pathways are essential for *S. agalactiae* neuropathogenesis.

Δ*aroA* elicited protective immune response against *S. agalactiae* in murine models

Before evaluating the potential of Δ*aroA* as a live attenuated vaccines, we assesed its genetic stability. The Δ*aroA* strain was subjected to 20 passages in vitro, and potential genetic changes were monitored through PCR analysis and sequencing. Results demonstrated that the *aroA* deletion region remained unchanged throughout all passages (Fig. S1).

We next evaluated the protective efficacy of Δ*aroA* in vaccination experiments. As shown in Fig. 6A, immunization with the Δ*aroA* at a dose of 1.0×10^3 CFU/mouse or higher achieved 100% RPS against a challenge with 10^2 CFU of the highly virulent GD201008-001 wild-type strain ($LD_{50} < 10$ CFU)[38]. All mice treated with PBS died within 48 h after challenge. With the increase of challenge doses, the protective efficacy with the 1.0×10^3 CFU/mouse dose of Δ*aroA* progressively declined, with RPS values of 90% (1.0×10^4 CFU/mouse), 70% (1.0×10^6 CFU/mouse) and 20% (1.0×10^8 CFU/mouse).

To further evaluate the Δ*aroA* vaccine candidate, we followed an established immunization protocol (Fig. 6B). Mice received two intraperitoneal (IP) injections at 0 and 28 days. All mice were divided into three groups including live Δ*aroA* (1.0×10^3 CFU/mouse), formalin-inactivated *S. agalactiae* whole cells (1.0×10^6 CFU/mouse), and PBS. At 42 dpi, mice were challenged with 10^4 CFU of wild-type *S. agalactiae* and monitored for 14 days. Strikingly, while the PBS control exhibited 100% mortality within 24 h after challenge, the Δ*aroA* group showed complete protection (0% mortality), significantly outperforming the inactivated group (60% mortality) (Fig. 6C).

Then we quantified specific antibody levels as determined by whole bacterial cell ELISA. Both Δ*aroA* and inactivated groups showed characteristic primary and secondary immune responses, with antibody titers peaking at 28 dpi, followed by a gradual decline. The Δ*aroA* group maintained significantly higher antibody levels throughout the observation period compared to the inactivated group ($P < 0.05$); in contrast, the PBS group maintained baseline antibody levels throughout the trial (Fig. 6D). Given the limited correlation between ELISA titers and protective immunity, we assessed functional antibody capacity using an opsonophagocytic assay (OPA). The Δ*aroA*-induced antiserum demonstrated significant, dose-dependent opsonophagocytic activity, compared to the naive serum, in the presence of murine macrophages RAW264.7 (Fig. 6E), confirming the elicitation of functional antibodies capable of mediating phagocytosis.

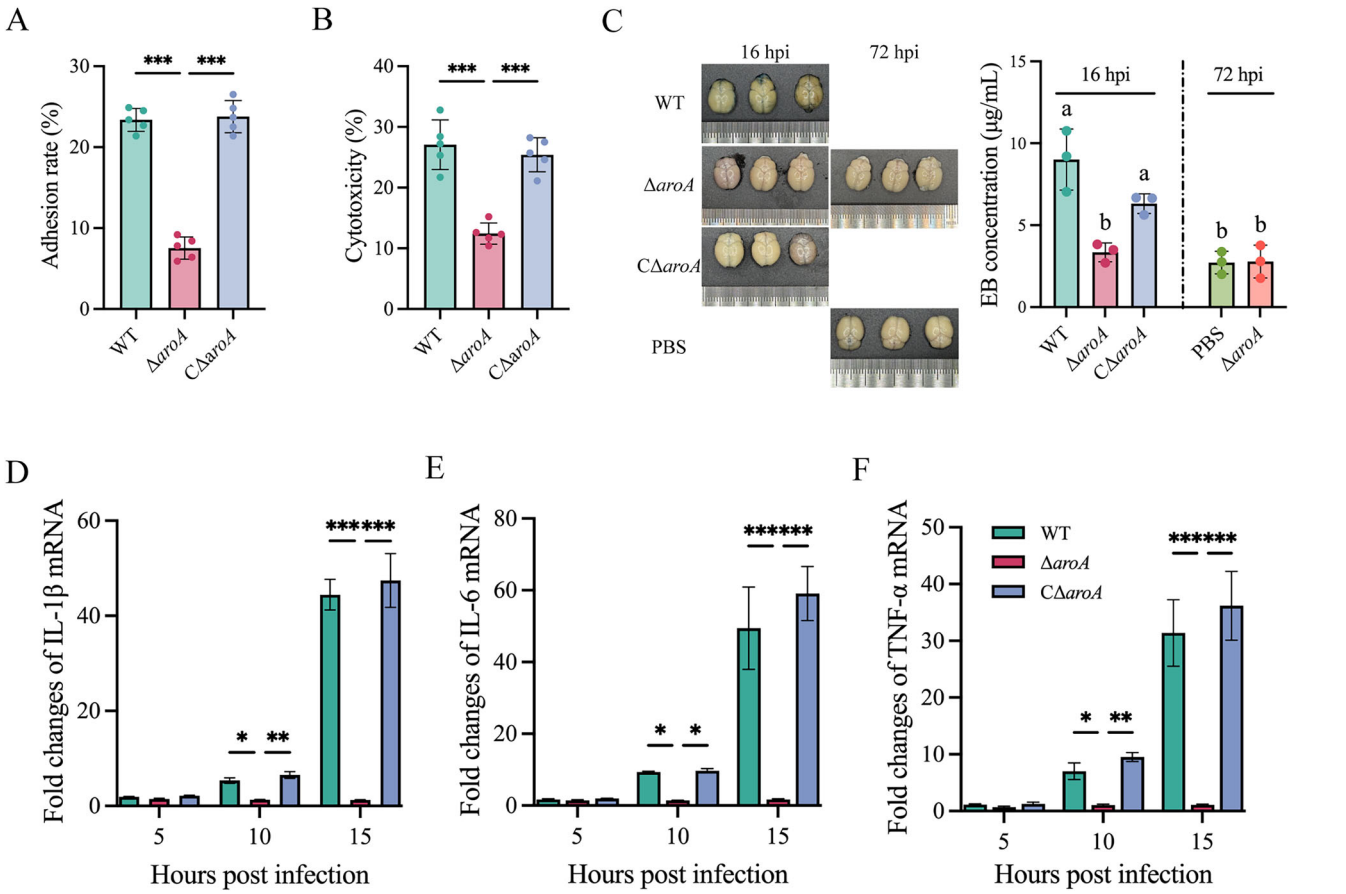

Fig. 5 | *aroA* contributes to *S. agalactiae* endothelial cell damage, blood-brain barrier disruption and induction of neuroinflammation. A Adhesion ability of the indicated strains to bEnd.3 cells. At 2 h postinfection, cells were washed and lysed for measurement of the number of CFU. **B** Bacterial cytotoxicity assessed by LDH release from RAW 264.7 macrophages after 4 h infection. C Evans Blue (EB) dye accumulation at 16 and 72 hpi to evaluate the permeability of the BBB ($n = 3$). Cerebral transcription levels of cytokines IL-1β (**D**), IL-6 (**E**), and TNF-α (**F**) in BALB/c mice infected with the indicated *S. agalactiae* strains ($n = 5$). Error bars represent SD. $^{*}P < 0.05$; $^{**}P < 0.01$; $^{***}P < 0.001$.

Also, we analyzed the cellular immune response in mice vaccinated with the Δ*aroA* and inactivated *S. agalactiae* whole cells. From 14 dpi on, the proportions of $CD4^{+}CD8^{-}$ (Fig. 7A) and $CD4^{-}CD8^{+}$ (Fig. 7B) T cells in splenic lymphocytes were significantly increased in the two vaccine immunization groups ($P < 0.01$ or $P < 0.001$), as compared with PBS group. The percentage of $CD4^{+}CD8^{-}$ cells peaked at 47.67% in the Δ*aroA* group at 35 dpi, while the peak value (42.31%) in the inactivated group was observed at 42 dpi. At 28 dpi, the percentage of $CD4^{+}CD8^{-}$ cells was significantly higher in the Δ*aroA* group compared to the inactivated group. Similarly, the percentage of $CD4^{-}CD8^{+}$ cells peaked at 35 dpi in both vaccine groups, with values of 22.96% and 17.29% in the Δ*aroA* and inactivated groups, respectively. From 21 to 56 dpi, the proportion of $CD4^{-}CD8^{+}$ cells remained a higher level in the Δ*aroA* group than in the inactivated group, and exhibted statistical differences ($P < 0.05$ or $P < 0.001$) between the two groups at most time points (21, 35, 49, and 56 dpi).

Next, the expression of IL-4 (Fig. 7C) and IFN-γ (Fig. 7D) in splenic lymphocytes of mice was accessed via qRT-PCR. In the Δ*aroA* group, both IL-4 and IFN-γ mRNA levels began to rise at 7 dpi. These levels peaked at 35 dpi for IL-4 and 42 dpi for IFN-γ, respectively. In contrast, in the inactivated group, IL-4 and IFN-γ expression started to increase at 14 dpi and 7 dpi, respectively, both peaking at 49 dpi. Notably, the IL-4 mRNA level was significantly higher in the Δ*aroA* group compared to the inactivated vaccine group at all tested time points (7, 14, 21, 28, 35, 42, 49, and 56 dpi). Similarly, IFN-γ expression was significantly elevated in the Δ*aroA* group at 7, 35, 42, and 56 dpi.

Together, our data indicate that the Δ*aroA* induced a robust and sustained immune response, whether humoral or cellular, suggesting the potential of the Δ*aroA* as a promising vaccine candidate.

Δ*aroA* provides robust protection against *S. agalactiae* in Nile tilapia

Considering that mice are not natural hosts for *S. agalactiae*, we systematically evaluated its protective efficacy against both homologous and heterologous challenge with *S. agalactiae* strains of sequence type 7 (ST7) and serotype Ia in Nile tilapia. Vaccination with the Δ*aroA* strain at doses of 1.0×10^{5} and 1.0×10^{6} CFU/fish elicited significant dose-dependent protection. Specifically, the 1.0×10^{6} CFU/fish dose provided 100% protection against homologous lethal challenge (GD201008-001) and 92.59% protection against heterologous challenge (BH4) (Fig. 8A). Serum IgM antibody levels were quantified by ELISA in fish vaccinated with a dose of 1.0×10^{6} CFU/fish at 1, 3, 7, 14, and 28 dpi. The results indicated that the Δ*aroA* strain elicited specific serum IgM antibodies as early as 3 dpi, with levels peaking at 7 dpi and maintaining elevated levels through at least 28 dpi (Fig. 8B).

Recognizing the practical potential of immersion vaccination, we evaluated the safety and protective efficacy of the Δ*aroA* strain administered via this route. Our results indicated that immersion vaccination with the Δ*aroA* strain at a dose of 1.0×10^{7} CFU/mL for 30 min caused no mortality, whereas a dose of 1.0×10^{8} CFU/mL resulted in a 13.33% mortality rate (Fig. 8C). Therefore, we selected the 1.0×10^{7} CFU/mL dose for 30-min immersion vaccination, which provided 50% protection against homologous lethal challenge and 42.86% protection against heterologous challenge (Fig. 8D).

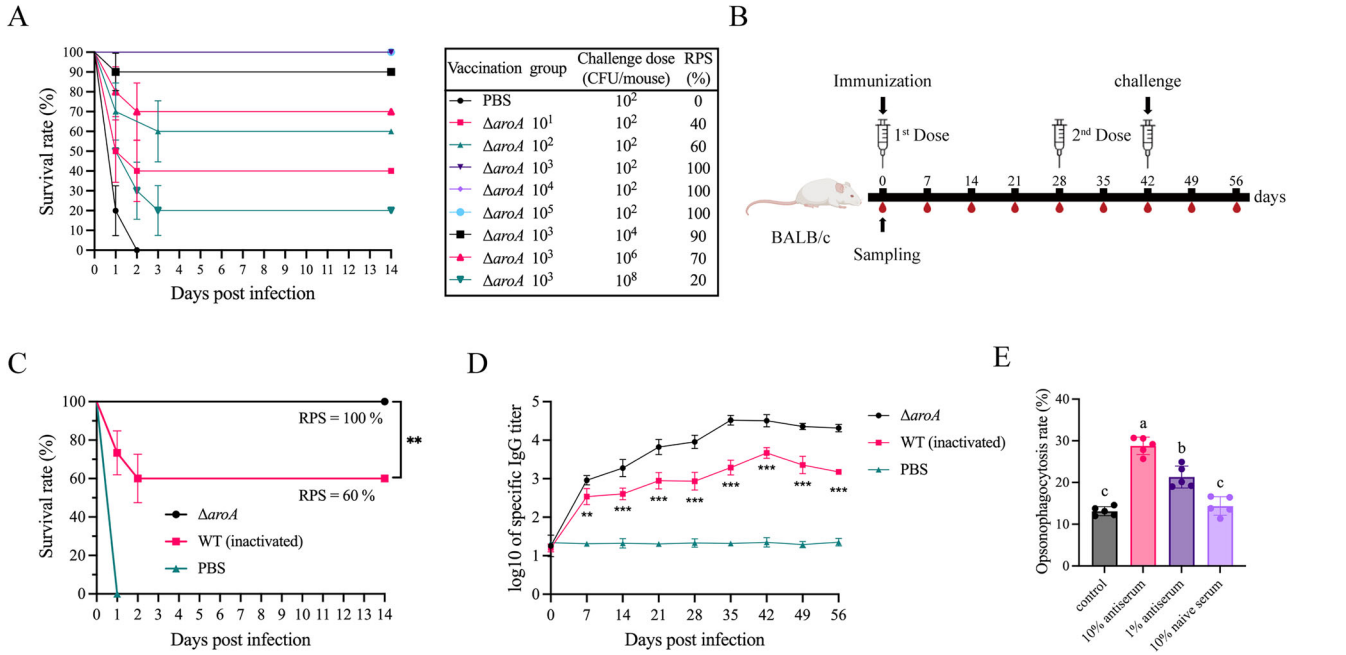

Fig. 6 | Immunization with the Δ*aroA* induces the humoral response in BALB/c mice. A Kaplan–Meier survival curve of mice immunized with different doses of Δ*aroA* ($n = 10$) following intraperitoneal challenge with 10^2–10^8 CFU/mouse of *S. agalactiae* GD201008-001 at 14 dpi. **B** Immunization protocol and sample collection timeline for BALB/c mice (PBS-injected controls included). **C** Kaplan–Meier survival curve of mice following intraperitoneal challenge with 10^4 CFU of the wild-type *S. agalactiae* GD201008-001 or Δ*aroA* ($n = 15$). **D** *S. agalactiae*-specific IgG antibody titers in serum of mice measured by whole-bacterial ELISA at the indicated time points ($n = 5$). **E** Opsonophagocytic activity assessed by bacterial uptake in RAW264.7 macrophages after 30 min serum opsonization and 1 h infection ($n = 5$). Error bars indicate SD. $^{**}P < 0.01$; $^{***}P < 0.001$. Different lowercase letters indicate statistically significant differences between groups ($P < 0.05$).

Discussion

The shikimate pathway is a well-validated antimicrobial target due to its absence in mammals while being essential for bacterial growth and virulence[43]. This metabolic pathway enables bacteria to synthesize aromatic amino acids (Phe, Trp and Tyr) de novo, which are critical for bacterial persistence in nutrient-limited host environments[44]. Among its key enzymes, EPSPS has been identified as a promising target for vaccine development[45], with deletion of *aroA* demonstrating strong protection against several pathogens[34,37,46]. However, the specific role of this pathway in *S. agalactiae* remained poorly characterized.

In this study, we demonstrated that the *aroA* gene is critical not only for GBS growth under nutrient-limited conditions and but also for its survival within macrophages. Notably, the growth defect of Δ*aroA* in macrophages could not be restored by supplementation with Phe, Trp, or Tyr, although the three amino acids are derived from chorismate, the end product of the shikimate pathway[40]. This observation contrasts with findings in *S. pneumoniae* and S. suis, where the shikimate pathway supports de novo synthesis of Tyr and Phe[47,48]. To elucidate this discrepancy, we conducted phylogenetic analysis of the shikimate pathway and downstream aromatic amino acid biosynthesis pathways across Streptococcaceae (Fig. S2). While most species retain complete genetic machinery for de novo chorismate biosynthesis, substantial interspecies heterogeneity exists in downstream aromatic amino acid biosynthesis pathways. Notably, *S. agalactiae* GD201008-001 harbors an incomplete *trpEGDCFBA* operon, retaining only *trpEG* encoding anthranilate synthase and thus lacking the capacity for de novo tryptophan synthesis[49,50]. Furthermore, we did not identify orthologs of *pheA*[51], *tyrA*[52] and *tyrB*[53], genes typically required for Phe and Tyr biosynthesis in many bacteria, suggesting alternative mechanisms for aromatic amino acid acquisition in *S. agalactiae*. Collectively, these features suggest that in this strain, the shikimate pathway may not be directly coupled to de novo production of Trp, Phe, or Tyr, which may help explain why exogenous amino acid supplementation failed to restore the intracellular survival defect of the Δ*aroA* under our experimental conditions. Further studies will be required to delineate the mechanism by which *aroA* contributes to bacterial intracellular survival in macrophages. Interestingly, Trp supplementation in infected macrophages led to a dose-dependent reduction in bacterial survival, implicating an important role of Trp metabolism as an innate antimicrobial mechanism. This aligns with reports that Trp catabolism serves as an innate immune defense mechanism, either through aryl hydrocarbon receptor (AhR)-mediated transcriptional reprogramming[54], or IFNγ-induced Trp depletion via kynurenine pathway activation[55,56].

To evaluate the virulence of Δ*aroA*, we used both zebrafish and Nile tilapia as model hosts. While the wild-type strain induced obvious neurological symptoms and meningitis-like pathological changes characteristic of fish streptococcosis[57,58], the Δ*aroA* strain caused no such symptoms. Given the high susceptibility of mice to this bacterium and their capacity to develop prominent neuropathological changes[59,60], we also employed a murine model to assess Δ*aroA* virulence. As expected, the *aroA* deletion impaired BBB crossing, reduced neuroinflammation, and mitigated pathological lesions, further confirming its attenuated phenotype. Notably, classical neuroinflammatory lesions, such as microglial nodules and prominent macrophage infiltrates[60], were absent in this mouse model, likely due to rapid systemic proliferation causing acute mortality before overt meningeal inflammation developed. Although we did not perform formal semi-quantitative scoring, qualitative assessment consistently showed markedly diminished neuroinflammation and pathology with Δ*aroA* compared to WT and CΔ*aroA* strains. This was further supported by significantly reduced expression levels of proinflammatory cytokines (IL-1β, IL-6, and TNF-α) in mouse brains. Although the precise mechanism by which Δ*aroA* reduced bacterial meningitis remains unclear, we speculate it may involve reduced metabolic capacity in brain tissue. It has been reported that *Streptococcus* spp. dynamically adjusts their metabolism to survive in diverse host environments, including nutrient-restricted sites like cerebrospinal fluid (CSF)[61,62]. Transcriptional profiling in *S. suis* reveals increased expression of shikimate pathway genes (*aroB*, *aroE*, *aroK*) in CSF, indicating their critical role in metabolic adaptation to the CSF environment[63]. The diminished neuroinflammation and pathological lesions observed with *varoA* may thus stem from its reduced capacity to adapt metabolically in the

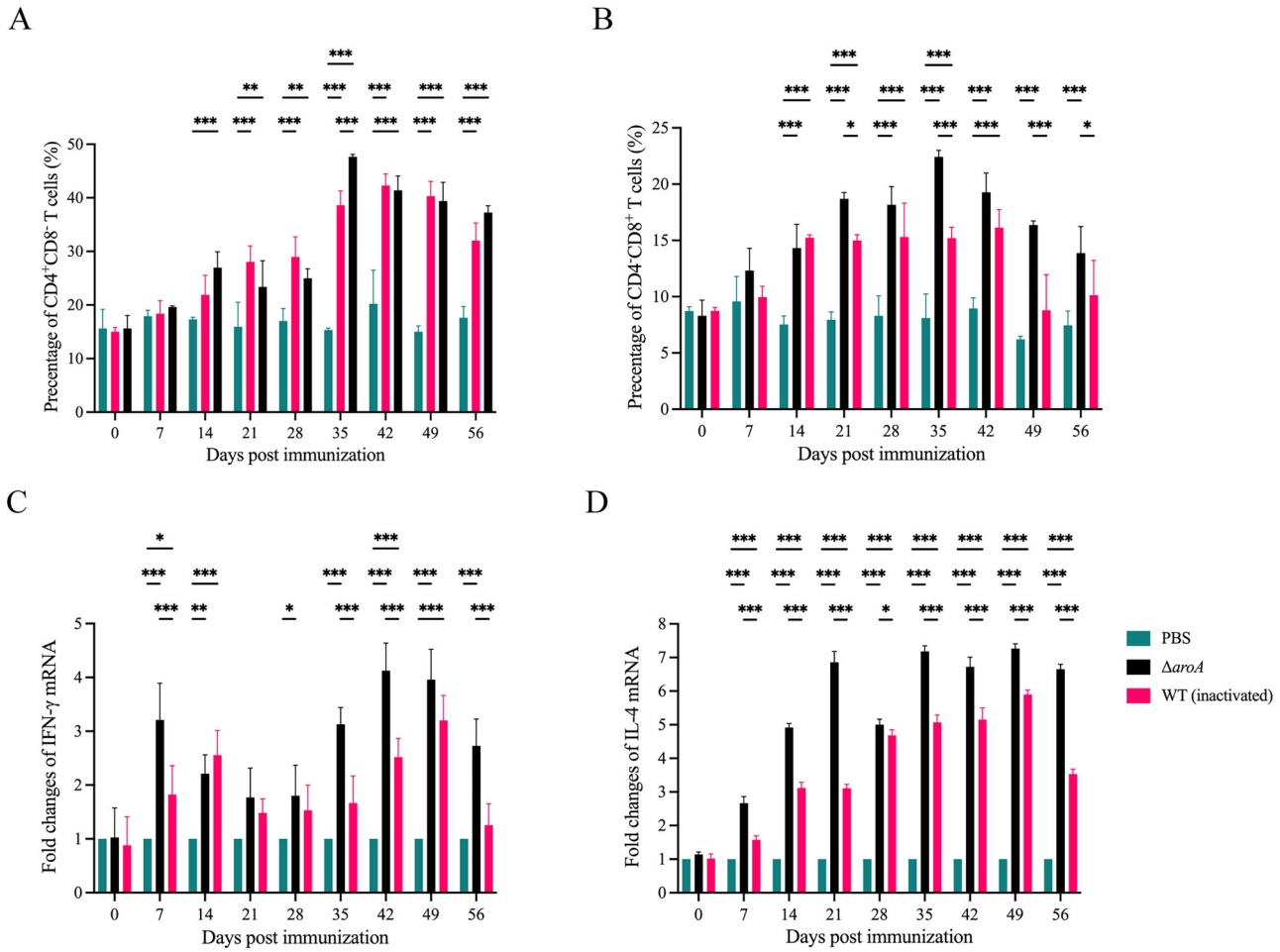

Fig. 7 | Immunization with Δ*aroA* induces the cellular response in BALB/c mice. Flow cytometric analysis of $CD4^+CD8^-$ T cells (**A**) and $CD4^-CD8^+$ T cells (**B**) populations in splenocytes from immunized and control mice at the indicated time points ($n = 5$). qRT-PCR analysis of IL-4 (**C**) and IFN-γ (**D**) mRNA expression in splenic lymphocytes post-immunization at the indicated time points ($n = 5$). Error bars represent SD. $^*P < 0.05$; $^{**}P < 0.01$; $^{***}P < 0.001$.

CSF. These findings collectively demonstrate that the deletion of *aroA* significantly impairs the ability of *S. agalactiae* to invade and damage the CNS, strongly supporting the safety of Δ*aroA* as a potential live attenuated vaccine candidate.

To enable a comprehensive immunological evaluation, we compared immune responses between the live attenuated Δ*aroA* strain and inactivated wild-type *S. agalactiae* vaccines using a murine model. This approach allowed us to utilize well-established immunological tools unavailable for teleost systems. The Δ*aroA* group exhibited significantly higher antibody levels and produced potent opsonophagocytic antibodies, a key correlate of protection for this extracellular pathogen[31]. Additionally, the Δ*aroA* vaccine elicited stronger effector T-cell responses, evidenced by increased $CD4^+$ and $CD8^+$ T cell production. $CD4^+$ T cells regulate humoral and cellular immunity via cytokine secretion[64], while $CD8^+$ T cells play an important role in eliminating infected cells[65]. This coordinated T cell response was further reflected in significantly elevated splenic lymphocyte expression of IFN-γ (Th1 marker) and IL-4 (Th2 marker) in the Δ*aroA* group compared to the inactivated group. These data demonstrate that the Δ*aroA* vaccine induces a more robust and durable immune response, encompassing both humoral and cellular components, which may enhance protective efficacy.

While the murine model provided valuable insights into the immunogenicity and protective efficacy of the Δ*aroA* strain, it is important to note that mice are not natural hosts for *S. agalactiae* in aquaculture. Therefore, we evaluated the vaccine potential of Δ*aroA* in its natural host, Nile tilapia, through the immunization-challenge experiment. We measured GBS-specific serum IgM antibodies, a key indicator of early humoral immunity[66], and found that Δ*aroA* immunization elicited significant humoral response against *S. agalactiae* infection. This observation is consistent with literature showing that a single immunization induced modest IgM levels in Nile tilapia, with peak titers typically detected within weeks post-inoculation[67]. Given the importance of opsonophagocytic antibodies in predicting protective immunity[31], we plan to develop an OPA assay using tilapia head-kidney phagocytes for future evaluation. Notably, the Δ*aroA* strain provided effective immune protection against both homologous and heterologous bacterial challenges via both immersion and intraperitoneal injection, though immersion offered weaker protection. Given the practical advantages of immersion vaccination[68], further protocol optimization is required to enhance protective efficacy in tilapia aquaculture[69].

Genetic stability and biosafety are critical considerations for live attenuated vaccines[70]. Our Δ*aroA* strain, engineered with a stable, complete gene deletion rather than a point mutation, presents an exceptionally low risk of reversion to virulence. This defined genetic design significantly reduces the potential for virulence regain through recombination with wild-type strains, as it would require a highly improbable homologous recombination event to restore the entire deleted sequence. Compared to the attenuated *S. agalactiae* WC1535 Δ*Sia* strain, which carries a deletion in the sialic acid synthesis cluster and demonstrates long-term colonization capacity, our Δ*aroA* strain exhibits a superior safety profile[71]. The metabolic auxotrophy attenuates bacterial virulence while inherently limiting persistence and transmissibility by imposing strict nutritional requirements that prevent sustained host colonization. This is supported by our experimental data showing complete pathogen clearance from Nile tilapia within 7 dpi

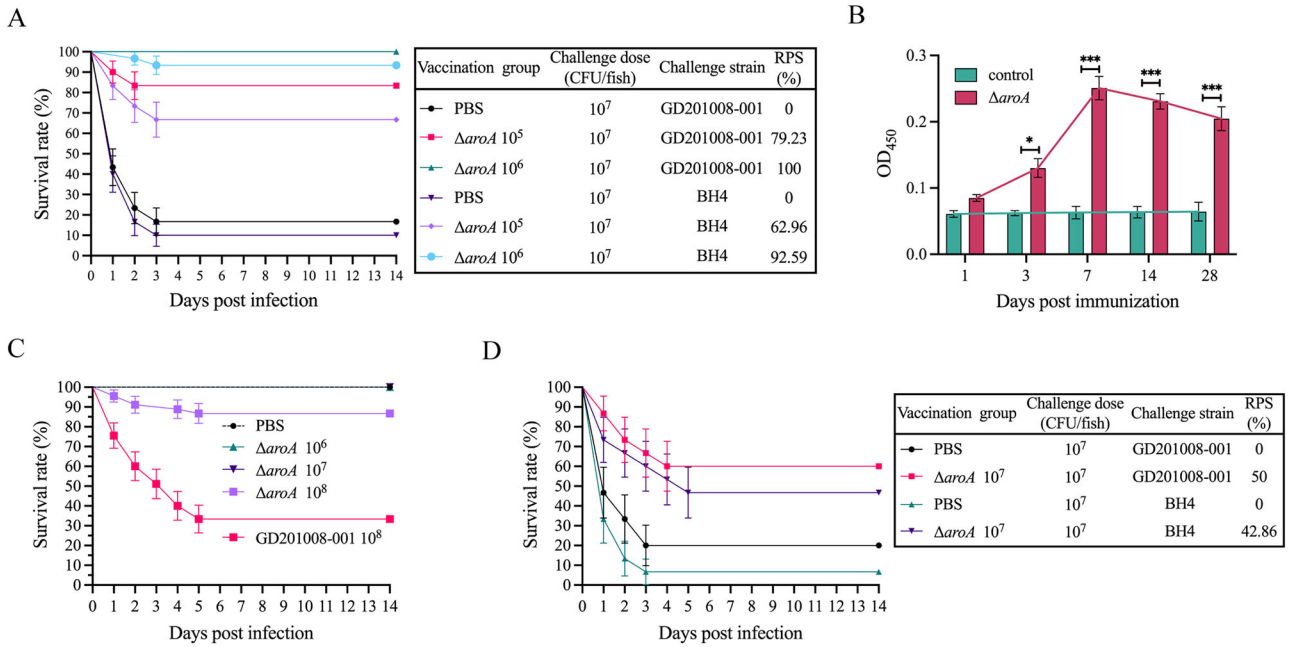

Fig. 8 | Immunization with the Δ*aroA* provides strong protective immunity against *S. agalactiae* infection in Nile tilapia. **A** Kaplan–Meier survival curve of Nile tilapia immunized with different doses of Δ*aroA* ($n = 30$) following intraperitoneal challenge with 10^7 CFU/fish of indicated *S. agalactiae* at 14 dpi. **B** *S. agalactiae*-specific IgM antibody titers in serum of Nile tilapia measured by whole-bacterial ELISA at the indicated time points ($n = 5$). **C** Kaplan–Meier survival analysis of tilapia following immersion challenge with *S. agalactiae* ($n = 45$). **D** Kaplan–Meier survival curve of Nile tilapia immunized with 10^7 CFU/fish of Δ*aroA* ($n = 15$) following immersion challenge with 10^7 CFU/fish of indicated *S. agalactiae* at 14 dpi. Error bars represent SD. $^{**}P < 0.01$; $^{***}P < 0.001$.

(Fig. S3), strongly suggesting limited environmental shedding and transmission potential.

While the Δ*aroA* live attenuated strain demonstrates robust immune protection and shows promise as a vaccine candidate, its applicability against the dominant circulating strains must be considered. Extensive surveillance in China has consistently shown that serotype Ia and genotype ST7 account for over 95% of piscine *S. agalactiae* isolates, particularly in tilapia outbreaks[10,72]. Therefore, a vaccine providing robust protection against this predominant lineage would address the vast majority of field cases. Our vaccine has demonstrated high efficacy against the dominant serotype Ia/ST7 strain in China. However, its efficacy against other, less common serotypes, e.g., Ib and III, requires empirical validation in future studies.

In conclusion, this study demonstrates that the Δ*aroA* exhibits stable attenuation and high immunogenicity, establishing its potential as an effective vaccine candidate against *S. agalactiae* in tilapia. Together with prior evidence from *aroA*/*phoP* mutants in *Edwardsiella piscicida*[73], our findings support the notion that attenuation of the shikimate pathway represents a promising strategy for developing live vaccines that balance safety and robust immunity across diverse fish pathogens. The Δ*aroA* approach aligns with the growing focus on metabolically attenuated live vaccines capable of inducing strong systemic and mucosal immune responses in fish[74]. Future studies will focus on the long-term protective efficacy and immune memory persistence of the vaccine, with a particular aim to elucidate the underlying T-cell activation pathways in Nile tilapia[75]. Additionally, we will further enhance vaccine safety by constructing double-deletion mutants, such as Δ*aroA*Δ*cpsE* or Δ*aroA*Δ*aroK* combinations, to eliminate any possibility of virulence reversion.

Methods

Ethics statement and animals

Five-week-old female BALB/c mice were purchased from the Experimental Animal Center of Yangzhou University. Zebrafish, with an average length of 1–2 cm, were provided by the Jiangsu Provincial Aquatic Animal Disease Prevention and Control Center. Nile tilapia, averaging 5–6 cm in length, were purchased from a commercial aquatic farm in Guangzhou, Guangdong Province, China. All experimental procedures involving animals were approved by the Ethical Committee for Animal Experiments of Nanjing Agricultural University, Nanjing, China. Efforts were made to minimize animal suffering and reduce the number of animals used while achieving scientific objectives.

Bacterial strains and cells

S. agalactiae strain GD201008-001 used in this study was originally isolated in 2010 from Nile tilapia exhibiting clinical signs of meningoencephalitis during an outbreak in Guangdong Province, China[12]; BH4 strain, also belonging to serotype Ia and multilocus sequence type (MLST) ST7, was originally isolated in 2019 from Nile tilapia (unpublished). Both strains were grown in Todd–Hewitt broth (THB) or Dulbecco's Modified Eagle Medium (DMEM) at 37 °C. *Escherichia coli* strain DH5α served as the host for plasmid propagation and cultured in Luria-Bertani (LB) broth or on LB agar medium at 37 °C. When necessary, antibiotics were used as the following final concentrations: 100 μg/mL spectinomycin or 10 μg/mL erythromycin for *S. agalactiae*, and 50 μg/mL spectinomycin or 50 μg/mL kanamycin for *E. coli*. The murine macrophage cell line RAW264.7 was maintained in DMEM supplemented with 10% fetal bovine serum (FBS; Gibco) at 37 °C in 5% CO_2. The murine brain microvascular endothelial cell bEnd.3 was cultured in DMEM supplemented with 15% FBS under the same conditions.

Construction of the mutant and complement strains

The marker-free, non-polar *aroA* gene deletion mutant strain Δ*aroA* and the complement strain CΔ*aroA* were generated as described previously[76]. Briefly, the upstream and downstream fragments of the *aroA* gene were amplified using the primers aroA-P1/P2 and aroA-P3/P4, listed in Table S1, which were then fused by overlap extension PCR using the aroA-P1/aroA-P4 primer pair. The resulting fusion fragments were purified and cloned into the *Eco*RI- digested thermosensitive suicide vectors pSET4s to generate the *aroA* deletion vector, pSET4s-aroA. The pSET4s-aroA were transformed into competent *S. agalactiae* GD201008-001 cells by electroporation at 2.35 kV, 200 Ω, and 25 μF, and plated on THB agar (1.5% wt/vol) with

100 μg/mL spectinomycin. Successful double-crossover mutagenesis of the Δ*aroA* was confirmed by temperature and antibiotic counter-selection, followed by verification through PCR and qRT-PCR. To generate the complement strain CΔ*aroA*, we constructed a plasmid pSET2-aroA containing an open reading frame of *aroA* in the pSET2 vector. The resulting plasmid pSET2-aroA was propagated in E. coli DH5α, and the plasmid was verified by DNA sequencing. The resulting plasmid was then electroporated into Δ*aroA* to generate the complement strain CΔ*aroA*.

Bacterial growth curve

For growth curve determination, overnight cultures of *S. agalactiae* were washed twice with sterile PBS and adjusted to an initial OD_{600} of 1.0. The standardized cultures were then diluted 1:100 in fresh THB or DMEM medium and incubated at 37 °C with shaking at 180 rpm. Bacterial growth was monitored by measuring the OD_{600} every 2 h from 2 h to 24 h.

RNA isolation and qRT-PCR

The total RNA of bacterial cells was extracted as described previously[77]. Briefly, log-phase *S.agalactiae* was collected, washed, and resuspended in lysis buffer (30 mM sodium acetate, 0.5% SDS, 1 mM EDTA, pH 5.5) and mechanically disrupted using Lysing Matrix B (MP Biomedicals). After centrifugation at 10,000 × *g* for 3 min, the supernatant was mixed with an equal volume of acid phenol (pH 5.5), incubated at 68 °C for 5 min, and subjected to phase separation by centrifugation at 13,000 × *g* for 12 min, at 15 °C. The aqueous phase was then mixed with two volumes of ethanol precipitation solution (30:1 ethanol:3 M sodium acetate, pH 6.5). RNA pellets obtained by centrifugation (13,000 × *g*, 30 min, 4 °C) were washed with ice-cold 70% ethanol, air-dried, and resuspended in nuclease-free water.

The brains of BALB/c mice were collected after intraperitoneally infected with 1.0×10^2 CFU/mouse at 5 hpi, 10 hpi, and 15 hpi ($n = 5$). Total RNAs of brain were extracted using the EZNA Total RNA Kit I (Omega Bio-tek, Norcross, GA, USA) according to the manufacturer's instructions. RNA integrity was verified by 1.2% agarose gel electrophoresis, and cDNA was synthesized using HiScript II Q RT SuperMix (Vazyme, Nanjing, China). qRT-PCR was performed using AceQ qPCR SYBR green master mix (Vazyme, Nanjing, China) on a StepOnePlus Real-Time PCR Systems (Applied Biosystems). The relative gene expression was quantified using the $2^{-\Delta\Delta CT}$ method, with *β-actin*[76] and *recA*[78] serving as internal reference genes for mouse tissues and bacterial samples, respectively. A post-hoc analysis of the reference gene's raw Cq values was performed using the geNorm algorithm within the R-based package NormqPCR.

LD_{50} determination in zebrafish and tilapia

The zebrafish and Nile tilapia used in this study were raised for over a week before being challenged. Log-phase *S.agalactiae* strains were washed and resuspended in sterile PBS. Fish were anesthetized with tricaine methanesulfonate (MS-222) and intraperitoneally injected (*i.p.*) with 20 μL of bacterial suspension for zebrafish or 50 μL of bacterial suspension for Nile tilapia, both containing 10-fold serially diluted bacterial suspensions. Each treatment group included 10 fish. Fish in the control group were injected with an equal volume of PBS. Mortality was monitored twice daily for the subsequent 7 days. The LD_{50} was determined using nonlinear regression analysis with a four-parameter log-logistic model in GraphPad Prism 10.4.1 (GraphPad Software, La Jolla, CA, USA)[79].

Murine infections

BALB/c mice were intraperitoneally infected with 1.0×10^2 CFU/mouse of the indicated strains and survival was monitored for 7 days postinfection ($n = 10$ per group). For the bacterial burden assay, at 16 hpi, brains, spleens, and blood ($n = 5$) were harvested, weighed, and homogenized in sterile PBS. The homogenate was serially diluted in PBS and plated to count the CFU after being overnight cultured.

Adhesion and cytotoxicity assays

Adhesion and cytotoxicity assays were performed as previously described[76]. For the adhesion assay, bEnd.3 cells were seeded into 24-well culture plates and allowed to adhere for 24 h. Log-phase *S.agalactiae* strains were washed and resuspended in fresh serum-free DMEM. Bacterial suspensions were then inoculated onto bEnd.3 cell monolayers at a multiplicity of infection (MOI) of 1:1 and incubated for 2 h at 37 °C in 5% CO_2. The infected cells were then washed five times with PBS and lysed with 1 mL of 0.02% (v/v) Triton X-100 (Sigma-Aldrich) in sterile distilled water for 10 min. The lysates were serially diluted in PBS and plated to count the CFUs after overnight incubation.

For the cytotoxicity assay, bEnd.3 cells were seeded into 96-well culture plates and allowed to adhere for 24 h. Bacteria were cultured and diluted as described above. The bacterial suspension was inoculated onto bEnd.3 cell monolayers at a MOI of 1:1. After centrifugation at 800 × *g* for 10 min, the plates were incubated for 4 h. Then, the CytoTox 96® non-radioactive cytotoxicity assay (Promega) was used to measure LDH levels according to the manufacturer's protocol.

S. agalactiae phagocytosis, intracellular survival and opsonophagocytic assays

The intracellular survival and phagocytosis assays were performed as described previously[80]. For the intracellular survival assay, RAW 264.7 cells were seeded into 24-well culture plates and allowed to adhere for 24 h. Log-phase *S.agalactiae* strains were washed and resuspended in fresh serum-free DMEM. Bacterial suspensions were then incubated with RAW264.7 at a MOI of 1:1 at 1 h at 37 °C in 5% CO_2. To determine the initial bacterial load, serial dilutions of the inoculum were plated onto THB agar and incubated overnight at 37 °C. Following five washes with sterile PBS to remove extracellular bacteria, the cells were treated with serum-free DMEM containing 1% penicillin-streptomycin (Sigma-Aldrich) for 1 h at 37 °C to eliminate any residual extracellular bacteria, establishing the zero-time point. At designated time intervals (0, 2, 4, 6, 8, and 24 h), the cells were lysed to release intracellular bacteria. The phagocytosis rate was calculated as the percentage of the bacterial load at time zero relative to the initial bacterial load. The intracellular survival rate was determined as the percentage of the bacterial load at each time point relative to that at time zero. For OPA, *S. agalactiae* GD201008-001 was opsonized by incubation with mouse serum at 37 °C for 30 min before performing the phagocytosis assay as described above.

Evans Blue (EB) analysis

BBB integrity was evaluated using EB extravasation assays as previously described[81]. Briefly, mice were intravenously administered 100 μL of 2% EB solution 30 min prior to sacrifice following infection with experimental strains ($n = 3$). Before tissue collection, animals were deeply anesthetized and systemically perfused with 10 mL heparinized saline (10 U/mL in 0.9% NaCl) via cardiac puncture. After perfusion, whole brains were promptly excised and photographed under standardized lighting conditions to document EB extravasation patterns. For quantitative assessment, brain tissues were incubated in 1 mL of formamide at 55 °C for 24 h to ensure complete EB extraction. EB concentration was determined spectrophotometrically by measuring the absorbance at 620 nm.

Assessment for protective efficacy of Δ*aroA* in mice

To determine the optimal immunization and challenge doses, we conducted preliminary dose-response experiments in BALB/c mice. Mice were randomly assigned to eight experimental groups and one control group ($n = 10$ per group). Experimental groups were immunized intraperitoneally with 100 μL bacterial suspensions containing 10^1–10^5 CFU of the Δ*aroA* strain, while the control group received an equivalent volume of sterile PBS. Following a 14-day immunization period, all mice were challenged intraperitoneally with graded lethal doses (10^2 or 10^4–10^8 CFU) of the GD201008-001 strain. The mortality

was monitored twice daily for 14 days. The RPS was calculated using the following formula:

$$\mathrm{RPS}(\%) = \left(1 - \frac{\text{mortality of vaccinated group}}{\text{mortality of control group}}\right) \times 100 \quad (1)$$

To assess immune efficiency, BALB/c mice were randomly assigned to three groups ($n = 55$ per group), including the WT inactivated vaccine, Δ*aroA* live attenuated vaccine, and PBS control. For the inactivated vaccine, log-phase *S. agalactiae* GD201008-001 was inactivated with 0.4% (v/v) formaldehyde for 24 h at 37 °C, with complete inactivation verified by plating on THB agar for 48 h. The inactivated bacteria were then washed and resuspended in PBS. The inactivated group received 100 μL 1.0×10^6 CFU/mL of inactivated bacteria with Freund's adjuvant (complete at 0 dpi, incomplete at 28 dpi), while the Δ*aroA* live attenuated group received 100 μL 1.0×10^3 CFU/mL of Δ*aroA* at 0 and 28 dpi. The control group received 100 μL of PBS. All immunizations were administered intraperitoneally. At 42 dpi, ten mice from each group were randomly selected and challenged intraperitoneally with 1.0×10^5 CFU/mouse of GD201008-001. Mortality was monitored twice daily for 14 days, and the RPS was calculated by formula (1). Serum and spleen samples were collected at the indicated time points (0, 7, 14, 21, 28, 35, 42, 49, and 56 dpi). Serum samples were used to measure IgG antibody titers, while spleen samples were used for lymphocyte isolation and immune-related gene expression analysis.

Assessment for protective efficacy of Δ*aroA* in Nile tilapia

To determine the protective efficacy of Δ*aroA* in Nile tilapia, we employed both intraperitoneal (IP) injection and immersion immunization routes. For IP protection assessment, fish were randomly assigned to two experimental groups and one control groups ($n = 60$ per group). Two experimental groups were immunized intraperitoneally with 50 μL of Δ*aroA* bacterial suspensions at doses of 1.0×10^5 CFU and 1.0×10^6 CFU, respectively. The control group received 50 μL of sterile PBS. After 14 days post-immersion, sixty fish from each group were randomly selected and divided into two groups ($n = 30$ per group). They were then challenged intraperitoneally with 1.0×10^7 CFU of *S. agalactiae* GD201008-001 or BH4, respectively. Mortality was monitored twice daily for 14 days, and RPS was calculated by formula (1). Serum samples were collected via caudal vein puncture at five time points (1, 3, 7, 14, and 28 dpi) from an extra 1.0×10^6 CFU group ($n = 5$ per time point).

To determine the optimal immunization doses, we conducted preliminary dose-response experiments. Fish were randomly divided into three experimental groups and two control groups ($n = 45$ per group). The immersion challenge was performed as described previously[82]. Experimental groups were subjected to 30-min immersion in the bacterial suspensions containing 10^6–10^8 CFU/mL of Δ*aroA*. Two control groups received 10^8 CFU/mL of GD201008-001 and sterile PBS, respectively. Mortality was monitored twice daily for 14 dpi. For immersion immunization, fish were acclimated in 20 g/L salinity for 5 min, followed by a 30-min immersion in the bacterial suspensions containing 10^7 CFU/mL of Δ*aroA* ($n = 30$) or sterile PBS ($n = 30$), respectively. After 14 days post-immersion, thirty fish from each group were randomly selected and divided into two group ($n = 15$ per group). They were then challenged intraperitoneally with 1.0×10^7 CFU of *S. agalactiae* GD201008-001 or BH4, respectively. Mortality was monitored twice daily for 14 days, and the RPS was calculated by formula (1).

Whole-bacterial ELISA for detecting anti-bacterial IgG in mice and IgM in tilapia

The whole-bacterial ELISA was performed as described previously with slight modifications[37]. Inactivated *S. agalactiae* GD201008-001 (1.0×10^9 CFU/mL in coating buffer) was used to coat 96-well microplates (Costar) overnight at 4 °C. After blocking with 10% FBS in PBST (PBS containing 0.05% Tween-20) for 2 h at 37 °C, serially diluted mouse sera, along with negative/blank controls, were added to each well and incubated for 2 h at 37 °C. Reactivity was measured by adding horseradish peroxidase (HRP)-conjugated rabbit anti-mouse IgG (H&L; Abcam) for 1 h at 37 °C, followed by detection with TMB substrate (Tiangen). The reaction was stopped with 2 M H_2SO_4, and absorbance was measured at 450 nm using a microplate reader (Tecan).

The serum level of anti-*S. agalactiae* IgM in tilapia was measured as previously described with slight modifications[83,84]. Briefly, following coated and blocked, 96-well microplates were incubated with 1:20 diluted tilapia serum samples in PBST for 2 h at 37 °C. A mouse anti-tilapia IgM monoclonal antibody (Biogoethe, Wuhan), diluted 1:1000, was used as the primary antibody, followed by HRP-conjugated rabbit anti-mouse IgG as the secondary antibody. The antibody level was determined by measuring the absorbance at 450 nm after reaction with TMB substrate.

Lymphocyte isolation, phenotype analysis and immune-related gene expression

For lymphocyte isolation, spleens were dissociated into single-cell suspensions by mechanical disruption through a 200-μm nylon mesh. After washing and centrifugation ($300 \times g$, 10 min), lymphocytes were resuspended in PBS and separated by density gradient centrifugation using lymphocyte separation medium (LSM; GE Healthcare) at $300 \times g$ for 15 min. The isolated lymphocytes were washed, resuspended in PBS at 1×10^7 cells/mL, and counted using an automated cell counter; viability was confirmed by trypan blue exclusion. For phenotypic analysis, 1×10^7 cells were stained for 30 min at room temperature in the dark with anti-mouse CD3-FITC together with either CD4-R-PE or CD8-R-PE (BioLegend). After lysing red blood cells and washing, samples were analyzed on a BD FACSCanto II flow cytometer and data processed with FlowJo (v10.7.1). For gene expression, the total RNA was extracted from 5×10^6 lymphocytes, and qRT-PCR was performed as described above. Primers for β-actin, IFN-γ, and IL-4 are listed in Table S1.

Statistical analysis

All data management and statistical analyses were performed using GraphPad Prism (version 10.4.1; GraphPad Software Inc., USA). Statistical differences in bacterial loads in tissues were assessed using an unpaired Student's *t*-test. For all parametric analyses, data normality was first verified using the Shapiro-Wilk test. Statistical differences in cell-based assays, EB extravasation assay, and opsonophagocytosis were analyzed using one-way ANOVA followed by Tukey's multiple comparisons test. Growth curves, intracellular survival assays, qRT-PCR data, whole-bacterial ELISA results, and flow cytometry measurements were analyzed using two-way ANOVA with Tukey's multiple comparisons test. Survival curves were compared using the log-rank (Mantel–Cox) test.

Data availability

The genomic data supporting Fig. S2 are available in the Figshare repository under accession code https://doi.org/10.6084/m9.figshare.30643841.

Received: 20 July 2025; Accepted: 28 January 2026;
Published online: 05 February 2026

References

1. Furfaro, L. L., Chang, B. J. & Payne, M. S. Perinatal Streptococcus agalactiae epidemiology and surveillance targets. *Clin. Microbiol. Rev.* **31**, e00049–00018 (2018).
2. Russell, N. J. et al. Maternal colonization with group B Streptococcus and serotype distribution worldwide: systematic review and meta-analyses. *Clin. Infect. Dis.* **65**, S100–S111 (2017).
3. Mahmmod, Y. S., Klaas, I. C., Katholm, J., Lutton, M. & Zadoks, R. N. Molecular epidemiology and strain-specific characteristics of Streptococcus agalactiae at the herd and cow level. *J. Dairy Sci.* **98**, 6913–6924 (2015).

4. El Tigani-Asil, E. T. A. et al. Gangrenous mastitis in dromedary camels in UAE caused by Streptococcus agalactiae. *BMC Vet. Res.* **16**, 174 (2020).
5. Geng, Y. et al. Streptococcus agalactiae, an emerging pathogen for cultured ya-fish, Schizothorax prenanti, in China. *Transbound. Emerg. Dis.* **59**, 369–375 (2012).
6. Leal, C. A. G., Queiroz, G. A., Pereira, F. L., Tavares, G. C. & Figueiredo, H. C. P. Streptococcus agalactiae sequence type 283 in farmed fish, Brazil. *Emerg. Infect. Dis.* **25**, 776–779 (2019).
7. Food and Agriculture Organization of the United Nations. Fisheries Department. The State of World Fisheries and Aquaculture. (Food and Agriculture Organization of the United Nations (2024).
8. Xiong, W., Guo, C., Gozlan, R. E. & Liu, J. S. Tilapia introduction in China: economic boom in aquaculture versus ecological threats to ecosystems. *Rev. Aquac.* **15**, 179–197 (2023).
9. Li, L. et al. Rare serotype occurrence and PFGE genotypic diversity of Streptococcus agalactiae isolated from tilapia in China. *Vet. Microbiol.* **167**, 719–724 (2013).
10. Zhang, D. F. et al. Epidemiological characteristics of Streptococcus agalactiae in tilapia in China from 2006 to 2020. *Aquaculture* **549**, 737724 (2022).
11. Wang, B. et al. Complete genome sequence of Streptococcus agalactiae ZQ0910, a pathogen causing meningoencephalitis in the GIFT strain of Nile tilapia (Oreochromis niloticus). *J. Bacteriol.* **194**, 5132–5133 (2012).
12. Liu, G., Zhang, W. & Lu, C. Complete genome sequence of Streptococcus agalactiae GD201008-001, isolated in China from tilapia with meningoencephalitis. *J. Bacteriol.* **194**, 6653 (2012).
13. Mian, G. F. et al. Aspects of the natural history and virulence of S. agalactiae infection in Nile tilapia. *Vet. Microbiol.* **136**, 180–183 (2009).
14. Hayes, K., O'Halloran, F. & Cotter, L. A review of antibiotic resistance in Group B Streptococcus: the story so far. *Crit. Rev. Microbiol.* **46**, 253–269 (2020).
15. Kimura, K. et al. First molecular characterization of group B streptococci with reduced penicillin susceptibility. *Antimicrob. Agents Chemother.* **52**, 2890–2897 (2008).
16. Metcalf, B. J. et al. Short-read whole genome sequencing for determination of antimicrobial resistance mechanisms and capsular serotypes of current invasive *Streptococcus agalactiae* recovered in the USA. *Clin. Microbiol. Infect.* **23**, 574.e7-574.e14 (2017).
17. Gong, X. et al. Genomic characterization and resistance features of Streptococcus agalactiae isolated from non-pregnant adults in Shandong. *China. J. Glob. Antimicrob. Resist.* **38**, 146–153 (2024).
18. Khan, U. B. et al. Genomic analysis reveals new integrative conjugal elements and transposons in GBS conferring antimicrobial resistance. *Antibiotics* **12**, 544 (2023).
19. Zhou, M., Li, Q., Yu, S., Han, H. & Osborne, N. J. Co-proliferation of antimicrobial resistance genes in tilapia farming ponds associated with use of antimicrobials. *Sci. Total Environ.* **887**, 164046 (2023).
20. Haenen, O. L. et al. Bacterial diseases of tilapia, their zoonotic potential and risk of antimicrobial resistance. *Rev. Aquac.* **15**, 154–185 (2023).
21. Micoli, F., Bagnoli, F., Rappuoli, R. & Serruto, D. The role of vaccines in combatting antimicrobial resistance. *Nat. Rev. Microbiol.* **19**, 287–302 (2021).
22. Evans, J. J., Klesius, P. H. & Shoemaker, C. A. Efficacy of *Streptococcus agalactiae* (group B) vaccine in tilapia (*Oreochromis niloticus*) by intraperitoneal and bath immersion administration. *Vaccine* **22**, 3769–3773 (2004).
23. Ma, T.-Y. et al. Evaluation of MarR-deleted *Streptococcus agalactiae* as a live-attenuated vaccine candidate for Nile Tilapia (*Oreochromis niloticus*). *Aquaculture* **612**, 743195 (2026).
24. Saba, A. O. et al. Development, application, efficacy, and future directions of vaccination against Streptococcus infections in tilapia: a systematic review and meta-analysis. Aquac. Res. 2025, 5521990 (2025).
25. Li, L. P. et al. Development of live attenuated Streptococcus agalactiae vaccine for tilapia via continuous passage in vitro. *Fish Shellfish Immunol* **45**, 955–963 (2015).
26. Zhang, D. et al. An effective live attenuated vaccine against *Streptococcus agalactiae* infection in farmed Nile tilapia (*Oreochromis niloticus*). *Fish Shellfish Immunol.* **98**, 853–859 (2020).
27. Liu, L., Lu, D. Q., Xu, J., Luo, H. L. & Li, A. X. Development of attenuated erythromycin-resistant *Streptococcus agalactiae* vaccine for tilapia (*Oreochromis niloticus*) culture. *J. Fish Dis.* **42**, 693–701 (2019).
28. Minor, P. D. Live attenuated vaccines: historical successes and current challenges. *Virology* **479**, 379–392 (2015).
29. Hoiseth, S. K. & Stocker, B. A. Aromatic-dependent *Salmonella typhimurium* are non-virulent and effective as live vaccines. *Nature* **291**, 238–239 (1981).
30. Garcia, P. et al. A highly-safe live auxotrophic vaccine protecting against disease caused by non-typhoidal *Salmonella* Typhimurium. *in mice. J. Microbiol. Immunol. Infect.* **56**, 324–336 (2023).
31. Cabral, M. P. et al. Design of live attenuated bacterial vaccines based on D-glutamate auxotrophy. *Nat. Commun.* **8**, 15480 (2017).
32. Pigula, M. et al. An unnatural amino acid dependent, conditional *Pseudomonas* vaccine prevents bacterial infection. *Nat. Commun.* **15**, 6766 (2024).
33. Dosselaere, F. & Vanderleyden, J. A metabolic node in action: chorismate-utilizing enzymes in microorganisms. *Crit. Rev. Microbiol.* **27**, 75–131 (2001).
34. Felgner, S. et al. aroA-deficient *Salmonella enterica* serovar Typhimurium is more than a metabolically attenuated mutant. *mBio* **7**, e01220–01216 (2016).
35. Buzzola, F. R., Barbagelata, M. S., Caccuri, R. L. & Sordelli, D. O. Attenuation and persistence of and ability to induce protective immunity to a *Staphylococcus aureus aroA* mutant in mice. *Infect. Immun.* **74**, 3498–3506 (2006).
36. Vivas, J. et al. The auxotrophic *aroA* mutant of *Aeromonas hydrophila* as a live attenuated vaccine against *A. salmonicida* infections in rainbow trout (*Oncorhynchus mykiss*). *Fish Shellfish Immunol.* **16**, 193–206 (2004).
37. Sereme, Y. et al. A live attenuated vaccine to prevent severe neonatal *Escherichia coli* K1 infections. *Nat. Commun.* **15**, 3021 (2024).
38. Guo, C. M. et al. Identification of genes preferentially expressed by highly virulent piscine *Streptococcus agalactiae* upon interaction with macrophages. *PLoS ONE* **9**, e87980 (2014).
39. Mir, R., Jallu, S. & Singh, T. P. The shikimate pathway: review of amino acid sequence, function and three-dimensional structures of the enzymes. *Crit. Rev. Microbiol.* **41**, 172–189 (2015).
40. Shende, V. V., Bauman, K. D. & Moore, B. S. The shikimate pathway: gateway to metabolic diversity. *Nat. Prod. Rep.* **41**, 604–648 (2024).
41. Prasad, R., Kapoor, R., Srivastava, R., Mishra, O. P. & Singh, T. B. Cerebrospinal fluid TNF-α, IL-6, and IL-8 in children with bacterial meningitis. *Pediatr. Neurol.* **50**, 60–65 (2014).
42. van Deuren, M. et al. The pattern of interleukin-1beta (IL-1beta) and its modulating agents IL-1 receptor antagonist and IL-1 soluble receptor type II in acute meningococcal infections. *Blood* **90**, 1101–1108 (1997).
43. Frlan, R. An evolutionary conservation and druggability analysis of enzymes belonging to the bacterial shikimate pathway. *Antibiotics* **11**, 675 (2022).
44. Han, Q., Phillips, R. S. & Li, J. Aromatic amino acid metabolism. *Front. Mol. Biosci.* **6**, 22 (2019).
45. Karki, H. S. & Ham, J. H. The roles of the shikimate pathway genes, *aroA* and *aroB*, in virulence, growth and UV tolerance of *Burkholderia glumae* strain 411gr-6. *Mol. Plant Pathol.* **15**, 940–947 (2014).

46. Priebe, G. P. et al. Construction and characterization of a live, attenuated *aroA* deletion mutant of *Pseudomonas aeruginosa* as a candidate intranasal vaccine. *Infect. Immun.* **70**, 1507–1517 (2002).
47. Willenborg, J. et al. Characterization of the pivotal carbon metabolism of *Streptococcus suis* serotype 2 under ex vivo and chemically defined in vitro conditions by isotopologue profiling. *J. Biol. Chem* **290**, 5840–5854 (2015).
48. Hartel, T. et al. Characterization of central carbon metabolism of *Streptococcus pneumoniae* by isotopologue profiling. *J. Biol. Chem.* **287**, 4260–4274 (2012).
49. Lott, J. S. The tryptophan biosynthetic pathway is essential for *Mycobacterium tuberculosis* to cause disease. *Biochem. Soc. Trans.* **48**, 2029–2037 (2020).
50. Bardowski, J., Ehrlich, S. D. & Chopin, A. Tryptophan biosynthesis genes in *Lactococcus lactis* subsp. lactis. *J. Bacteriol.* **174**, 6563–6570 (1992).
51. Prakash, P., Pathak, N. & Hasnain, S. E. *pheA* (Rv3838c) of *Mycobacterium tuberculosis* encodes an allosterically regulated monofunctional prephenate dehydratase that requires both catalytic and regulatory domains for optimum activity. *J. Biol. Chem.* **280**, 20666–20671 (2005).
52. Ku, H. K. et al. Crystal structure of prephenate dehydrogenase from *Streptococcus mutans*. *Int. J. Biol. Macromol.* **49**, 761–766 (2011).
53. Shin, M. H. et al. X-ray structure of prephenate dehydratase from *Streptococcus mutans*. *J. Microbiol.* **52**, 490–495 (2014).
54. Keskey, R. C. et al. Enterobactin inhibits microbiota-dependent activation of AhR to promote bacterial sepsis in mice. *Nat. Microbiol.* **10**, 388–404 (2025).
55. Nino-Castro, A. et al. The IDO1-induced kynurenines play a major role in the antimicrobial effect of human myeloid cells against *Listeria monocytogenes*. *Innate Immun.* **20**, 401–411 (2014).
56. Ganesan, S. & Roy, C. R. Host cell depletion of tryptophan by IFNgamma-induced Indoleamine 2,3-dioxygenase 1 (IDO1) inhibits lysosomal replication of *Coxiella burnetii*. *PLoS Pathog* **15**, e1007955 (2019).
57. Palang, I., Withyachumnarnkul, B., Senapin, S., Sirimanapong, W. & Vanichviriyakit, R. Brain histopathology in red tilapia *Oreochromis* sp. experimentally infected with *Streptococcus agalactiae* serotype III. *Microsc. Res. Tech.* **83**, 877–888 (2020).
58. Pinho-Ribeiro, F. A. et al. Bacteria hijack a meningeal neuroimmune axis to facilitate brain invasion. *Nature* **615**, 472–481 (2023).
59. Dong, Y. et al. CRISPR-dependent endogenous gene regulation is required for virulence in piscine *Streptococcus agalactiae*. *Emerg. Microbes Infect.* **10**, 2113–2124 (2021).
60. Nie, M. et al. CRISPR contributes to adhesion, invasion, and biofilm formation in *Streptococcus agalactiae* by repressing capsular polysaccharide production. *Microbiol. Spectr.* **10**, e02113–e02121 (2022).
61. Schiavolin, L., Deneubourg, G., Steinmetz, J., Smeesters, P. R. & Botteaux, A. Group A *Streptococcus* adaptation to diverse niches: lessons from transcriptomic studies. *Crit. Rev. Microbiol.* **50**, 241–265 (2024).
62. Dresen, M., Valentin-Weigand, P. & Berhanu Weldearegay, Y. Role of metabolicadaptation of *Streptococcus suis* to host niches in bacterial fitness and virulence. *Pathogens* **12**, 541 (2023).
63. Koczula, A. et al. Transcriptomic analysis reveals selective metabolic adaptation of *Streptococcus suis* to porcine blood and cerebrospinal fluid. *Pathogens* **6**, 7 (2017).
64. Künzli, M. & Masopust, D. CD4+ T cell memory. *Nat. Immunol.* **24**, 903–914 (2023).
65. Kok, L., Masopust, D. & Schumacher, T. N. The precursors of CD8+ tissue resident memory T cells: from lymphoid organs to infected tissues. *Nat. Rev. Immunol.* **22**, 283–293 (2022).
66. Queiróz, G. A. D., Silva, T. M. F. E. & Leal, C. A. G. Duration of protection and humoral immune response in Nile tilapia (*Oreochromis niloticus* L.) vaccinated against Streptococcus agalactiae. *Animals* **14**, 1744 (2024).
67. Hao, J. et al. Construction of *Streptococcus agalactiae* sialic acid mutant and evaluation of its potential as a live attenuated vaccine in Nile tilapia (*Oreochromis niloticus*). *J. Appl. Microbiol.* **133**, 2403–2416 (2022).
68. Thompson, K. D. et al. Addressing nanovaccine strategies for tilapia. *Vaccines* **11**, 1356 (2023).
69. Linh, N. V. et al. Pre-treatment of Nile tilapia (*Oreochromis niloticus*) with ozone nanobubbles improve efficacy of heat-killed Streptococcus agalactiae immersion vaccine. *Fish Shellfish Immunol.* **123**, 229–237 (2022).
70. Frey, J. Biological safety concepts of genetically modified live bacterial vaccines. *Vaccine* **25**, 5598–5605 (2007).
71. Hao, J. et al. Attenuated *Streptococcus agalactiae* WC1535 ΔSia perturbs the gut microbiota of *Oreochromis niloticus*, massively colonizes the intestine, and induces intestinal mucosal immunity after intraperitoneal inoculation. *Front. Microbiol.* **13**, 1036432 (2022).
72. Chen, M. et al. PCR detection and PFGE genotype analyses of streptococcal clinical isolates from tilapia in China. *Vet. Microbiol.* **159**, 526–530 (2012).
73. Swain, B., Powell, C. T. & Curtiss, R. Virulence, immunogenicity and live vaccine potential of *aroA* and *phoP* mutants of *Edwardsiella piscicida* in zebrafish. *Microb. Pathog.* **162**, 105355 (2022).
74. Rathor, G. S. & Swain, B. Advancements in fish vaccination: current innovations and future horizons in aquaculture health management. *Appl. Sci.* **14**, 5672 (2024).
75. Li, K. et al. Fish requires FasL to facilitate CD8+ T-cell function and antimicrobial immunity. *J. Immunol.* **214**, 1219–1235 (2025).
76. Ma, K. et al. cas9 enhances bacterial virulence by repressing the regR transcriptional regulator in *Streptococcus agalactiae*. *Infect. Immun.* **86**, e00552–00517 (2018).
77. Oh, E. T. & So, J.-S. A rapid method for RNA preparation from Gram-positive bacteria. *J. Microbiol. Methods* **52**, 395–398 (2003).
78. Florindo, C. et al. Selection of reference genes for real-time expression studies in *Streptococcus agalactiae*. *J. Microbiol. Methods* **90**, 220–227 (2012).
79. Peng, X., Lei, C. & Sun, X. Comparison of lethal doses calculated using Logit/Probit–log (dose) regressions with arbitrary slopes using R. *J. Econ. Entomol.* **114**, 1345–1352 (2021).
80. Cao, Q. et al. Role of *luxS* in immune evasion and pathogenicity of piscine *Streptococcus agalactiae* is not dependent on autoinducer-2. *Fish Shellfish Immunol.* **99**, 274–283 (2020).
81. Pan, F. et al. Membrane vesicle delivery of a streptococcal M protein disrupts the blood-brain barrier by inducing autophagic endothelial cell death. *Proc. Natl. Acad. Sci. USA* **120**, e2219435120 (2023).
82. Ke, X. et al. The immune efficacy of a *Streptococcus agalactiae* immersion vaccine for different sizes of young tilapia. *Aquaculture* **534**, 736289 (2021).
83. Mo, X.-B., Wang, J., Guo, S. & Li, A.-X. Potential of naturally attenuated *Streptococcus agalactiae* as a live vaccine in Nile tilapia (*Oreochromis niloticus*). *Aquaculture* **518**, 734774 (2020).
84. Vinh, N. T. et al. Immunological response of 35 and 42 days old Asian seabass (*Lates calcarifer*, Bloch 1790) fry following immersion immunization with *Streptococcus iniae* heat-killed vaccine. *Fish Shellfish Immunol.* **138**, 108802 (2023).

Acknowledgements

This work was supported by the Joint Funds of the National Natural Science Foundation of China (U23A20254), Key Talent Programs in Key Industries of Jiangsu Province, "Qinglan Project" of Colleges and Universities in Jiangsu Province([2025] No. 16) and Postgraduate Research & Practice Innovation Program of Jiangsu Province (SJCX23_0220).

Author contributions

Y.L. supervised the research project, designed the study, and interpreted experimental results. M.N and Y.L wrote the main manuscript text. M.N. and C.G. conducted the majority of experiments and performed data analysis.

Y.D., T.X., and Y.S. provided technical assistance and experimental materials. Y.L. serves as the lead contact for correspondence. All authors critically reviewed and approved the final manuscript.

Competing interests
The authors declare no competing interests.

Additional information
Supplementary information The online version contains supplementary material available at https://doi.org/10.1038/s41541-026-01393-0.

Correspondence and requests for materials should be addressed to Yongjie Liu.